Hybrid Physics and Data-driven Contingency Filtering for Security Operation of Micro Energy-water Nexus

Mostafa Goodarzi and Qifeng Li, *Senior Member IEEE*

***Abstract*—This paper investigates a novel engineering problem, i.e., security-constrained multi-period operation of micro energy-water nexuses. This problem is computationally challenging because of its high nonlinearity, nonconvexity, and large dimension. We propose a two-stage iterative algorithm employing a hybrid physics and data-driven contingency filtering (CF) method and convexification to solve it. The convexified master problem is solved in the first stage by considering the base case operation and binding contingencies set (BCS). The second stage updates BCS using physics-based data-driven methods, which include dynamic and filtered data sets. This method is faster than existing CF methods because it relies on offline optimization problems and contains a limited number of online optimization problems. We validate effectiveness of the proposed method using two different case studies: the IEEE 13-bus power system with the EPANET 8-node water system and the IEEE 33-bus power system with the Otsfeld 13-node water system.**

***Index Terms*—Contingency filtering, micro energy-water nexus, multi-period secure operation, optimal power and water flow, physics-guided data-driven.**

NOMENCLATURE

A. Parameters

η	Constant efficiency of the pump.
Γ	Data sets.
ξ	Boundary values for contingency classification.
ρ	Cost constants for power generators.
ρ_t^{G}	Electricity price.
ϑ	Weight factor for physical information.
A_n^{T}	Water tank area at node n.
c, N_{B}	Contingency number, total number of buses.
D_{nm}, L_{nm}	Diameter and length of pipe.
$d_{n,t}$	Water demand of node n.
f_s	Darcy–Weisbach friction factor for water pipe.
g	Gravitational acceleration.
h_{nm}	Elevation difference among of node n and m.
N_{ds}	Number of data in the data set.
$P_{i,t}^{\mathrm{RE}}, Q_{i,t}^{\mathrm{RE}}$	Active/reactive power output of renewable energy.
PR	Maximum reduced pressure value.
r_{ij}	Resistance of the line between bus i and bus j.
R_{nm}^{w}	Head loss coefficient of pipe nm.
S_{ij}	Apparent power of the line between bus i and j.
x_{ij}	Reactance of the line between bus i and bus j.
z_{ij}	Impedance of the line between bus i and bus j.

B. Variables

α_{nm}^{P}	Binary variable shows the pump status.
μ_{ij}^c	Binary variable of the network reconfiguration.
γ^c	Violation value of contingency c.
ω	Weight factors.
$\tilde{d}_n^{\mathrm{p},c}, \tilde{d}_n^{\mathrm{n},c}$	Positive and negative water mismatch at node n.
f_{nm}^c	Water flow in the pipe between node n and m.
F_n^{R}	Water flow inject of the water source at node n.
$\tilde{F}_n^{\mathrm{R},c}$	Change in water production at node n.
$F_n^{\mathrm{T},c}$	Net water flow of tank at node n.
$\mathcal{I}_{ij}^c$	Square of the current magnitude.
$P_i^{\mathrm{ES}}, Q_i^{\mathrm{ES}}$	Active and reactive power of energy storage.
$P_i^{\mathrm{L}}, Q_i^{\mathrm{L}}$	Active and reactive power load.
P_{ij}^c, Q_{ij}^c	Active and reactive power flow.
$P_i^{\mathrm{g}}, Q_i^{\mathrm{g}}$	Active and reactive grid/DG power.
$\tilde{P}_i^{\mathrm{g},c}, \tilde{Q}_i^{\mathrm{g},c}$	Changes in grid/DG power generation.
$\tilde{P}_i^{\mathrm{p},c}, \tilde{P}_i^{\mathrm{n},c}$	Positive and negative power mismatch.
P_i^{pump}	Power demand of pump.
$\mathcal{V}_i^c$	Square voltage.
$V_n^{\mathrm{T},c}$	Water tank volume at node n.
$y_{nm}^{\mathrm{G},c}$	Head gains imposed by the pump in the pipe.
y_n^c	Water head of the node n.
$y_n^{\mathrm{T},c}$	Water head of the tank in the node n.

I. INTRODUCTION

POWER distribution networks (PDNs) must be secured by considering contingencies and taking corrective action (CA) and preventive action. Most power contingency research focuses on transmission, due to longer recovery times and potential cascading failures associated with transmission incidents. PDN is often vulnerable to severe weather, and it is estimated that up to 80% of all outages originate at the distribution level [1]. Moreover, as distributed generation increases and more microgrids are utilized, contingencies in a distribution

Manuscript received October 24, 2022; revised December 25, 2022; accepted February 16, 2023. Date of online publication April 20, 2023; date of current version May 17, 2023. This work was supported by U.S. National Science Foundation under Award no. 2124849.

M. Goodarzi and Q. F. Li (corresponding author, email: qifeng.li@ucf.edu) are with the Department of Electrical and Computer Engineering, University of Central Florida, Orlando, FL 32816 USA.

DOI: 10.17775/CSEEJPES.2022.07240

system may result in unexpected load shedding. Hence, it is necessary to study secure operations at the distribution level.

Modern-day water and power distribution systems are closely coupled, especially in small communities such as campuses of industrial parks, universities and labs, small islands, and remote villages. Their interdependence is increasing due to proliferation of electricity-driven water facilities (EDWFs). During a PDN contingency, such as loss of a power line, the water distribution system (WDS) may not function properly due to a lack of power feeding the EDWFs. The WDS will have to adjust its schedule, such as pump scheduling. WDS contingencies, like a water pump failure, could also impact EDWF operations and power consumption, affecting PDN security. This paper develops an optimization model of an $N-1$ security-constrained operation with corrective actions of the micro energy-water nexus (SOC-MEWN) to address such security problems.

Three control measures ensure MEWN's secure operation. Distribution network reconfiguration is adopted as the primary CA, due to the radial structure of the PDN. Although line switching may cause instability issues in transmission systems, it is reasonable to assume the grid-connected PDN has sufficient stability during line switching. Modification of grid power/controllable distributed generation (DG) power, as well as changes in water production, can be viewed as a secondary CA to control contingencies not covered by the primary CA. Changes in water production will change power consumption of WDS, making the PDN more resilient to address contingencies. Preventive action should be considered in the event of uncontrollable contingencies (UCs), which are contingencies that cannot be controlled by CAs. Preventive action may include 24-hour modification of grid power/controllable DG power and water production.

The SOC-MEWN problem is a multi-period security-constrained optimization problem for two complex networks, namely PDN and WDS. Therefore, this is a large-scale, mixed-integer, nonlinear, and nonconvex optimization problem that is computationally intractable and difficult to solve. Network reconfiguration should also be considered to reconnect isolated downstream customers in a contingency situation [2] due to PDN's radial structure [3]. These make SOC-MEWN a more challenging problem than security-constrained optimization problems of a single network. Although there exists limited research on the SOC-MEWN problem, security-constrained optimization problems of power systems have been studied for decades [4]–[6]. A comprehensive review of the power system security-constrained optimization problem can be found in [4]. Even though [5] proposes $N-1$ security-constrained optimal power and gas flow by considering two different systems, they did not account for multi-periodic operations. [6] suggests an $N-1$ security-constrained optimal power flow within a radial network, but it does not consider reconfiguration during a line failure, so its solution method may not fit all SOC-MEWN problems.

Many studies have proposed various methods for solving security-constrained optimization problems. A well-known approach involves an iterative algorithm with contingency filtering (CF). As most of the contingencies, at least 95% [7], are redundant for security operations in real-world systems, only a limited subset of contingencies needs to be considered, leading to significant reduction in computation time. The challenge resides in identifying these contingencies. Existing CF methods, such as ranking of CAs [8], binding contingencies [9], key contingencies [10], umbrella contingencies [11], and risk of failure of CAs [12], must solve an online optimization problem for each contingency in every iteration, which is time-consuming. Besides, these methods rely solely on physics-based models and may lead to nonconvex optimization problems that are computationally expensive [13]. We propose a two-level physics-guided data-driven (PGDD) method to avoid such problems and identify UCs quickly without solving any online optimization problems.

Machine learning (ML) techniques have been widely applied in power systems, as discussed in [14]. However, there exists limited research on using ML for CF. For contingency classifications in a MEWN, supervised ML methods such as decision trees (DT), support vector machines (SVM), naive Bayes (NB), and k-nearest neighbors (KNN) can be used. This paper evaluates performance of these supervised ML classification methods to find the best one for determining the UCs. The proposed PGDD model combines physics and data to increase accuracy and prevent overfitting that occurs with pure machine learning. We also develop dynamic and filtered data sets by adjusting weight factors for the conventional data set according to physical information such as environmental data.

In this study, we develop a two-stage iterative approach, employing both the proposed PGDD-CF method and a novel convexification technique to solve the SOC-MEWN problem, as shown in Fig. 1. The first stage (blue box) finds the solution of the convexified multi-period optimal power and water flow in the MEWN subject to the base-case operation constraints and binding contingencies set (BCS). In the second stage (light green box), the PGDD module classifies contingencies into three classes and finds the set of UCs. Then, the binding contingency filtering module (BCFM) specifies worst-case contingency from the UCs and adds it to the BCS for the next iteration. The updated BCS will change scheduled operation to obtain optimal secure operation in the upcoming iteration. Therefore, the PGDD and the BCFM will identify a new set of UCs and worst-case contingency. Iteration stops when no UC is found. The main contributions of this paper are:

- We have built a mathematical model for SOC-MEWN to improve security of MEWNs by considering power and water as one integrated system. The SOC-MEWN guarantees $N-1$ secure operation at a lower cost than if each system had a separate secure optimal operation.
- In contrast to the existing CF method, the proposed PGDD approach employs both data-driven and physics to classify contingencies, making it possible to identify UCs quickly by solving a limited number of online optimization problems.
- A novel convexification technique, i.e., the convex hull relaxation, is adopted to further improve computational efficiency of PGDD-CF-based SOC-MEWN without impacting analysis outcome.

The rest of this paper is organized as follows. Section II presents details of problem formulation. Section III introduces the solution method, including relaxation of the non-convex constraints and the proposed PGDD-CF approach. Section IV presents two case studies to validate this method. Finally, conclusions are drawn in Section V.

II. Problem Formulation

MEWN, which refers to energy and water systems in small communities, such as industrial parks, university campuses, small islands, and remote villages, can be controlled by a single entity. In these small communities, grid power meets most power demand, and DGs meet the rest. In this section, we develop an optimization formulation for the SOC-MEWN problem to minimize cost of secure operation. The MEWN model consists of two elements: the PDN and the WDS. Besides, EDWFs in both systems serve as a link between them. Fig. 2 illustrates a schematic of a typical MEWN [15]. WDS is shown in blue, PDN is in green, and the connection between them is shown with green dashed lines are EDWF, which will vary for different small communities. We will discuss the detailed model of this system in the following subsections. We consider the pump as EDWF in this paper, whereas other EDWF models can be found at [15].

A. Power Distribution Network

The well-known Distflow model is adopted to formulate power flow in the distribution system [16], [17]. A contingency will isolate all downstream customers of the on-contingency line in a radial structure. This paper uses reconfiguration as a primary CA to avoid loss of loads under contingency conditions. Besides, we consider an acceptable change in grid power/controllable DG power as a secondary CA in our model. Formulations are expressed by:

$$P^{\mathrm{g}}_{i,t} + P^{\mathrm{RE}}_{i,t} + P^{\mathrm{ES}}_{i,t} + \tilde{P}^{\mathrm{g},c}_{i,t} - P^{\mathrm{L}}_{i,t} = r_{ij}\mathcal{I}^{c}_{ij,t} - P^{c}_{ji,t} + \sum_{k} P^{c}_{ki,t} \tag{1a}$$

$$Q^{\mathrm{g}}_{i,t} + Q^{\mathrm{RE}}_{i,t} + Q^{\mathrm{ES}}_{i,t} + \tilde{Q}^{\mathrm{g},c}_{i,t} - Q^{\mathrm{L}}_{i,t} = x_{ij}\mathcal{I}^{c}_{ij,t} - Q^{c}_{ji,t} + \sum_{k} Q^{c}_{ki,t} \tag{1b}$$

$$\widehat{\mathcal{V}} = 2(r_{ij}P^{c}_{ij,t} + x_{ij}Q^{c}_{ij,t}) - z^{2}_{ij}\mathcal{I}^{c}_{ij,t} \tag{1c}$$

$$(P^{c}_{ij,t})^2 + (Q^{c}_{ij,t})^2 = \mathcal{V}^{c}_{i,t}\mathcal{I}^{c}_{ij,t} \tag{1d}$$

$$(P^{c}_{ij,t})^2 + (Q^{c}_{ij,t})^2 \le \overline{S_{ij}}^{2} \tag{1e}$$

$$0, \underline{\mathcal{V}_i}, \underline{P^{\mathrm{g}}_i}, \underline{Q^{\mathrm{g}}_i} \le \mathcal{I}^{c}_{ij,t}, \mathcal{V}^{c}_{i,t}, P^{\mathrm{g}}_{i,t}, Q^{\mathrm{g}}_{i,t} \le \overline{\mathcal{I}_{ij}}, \overline{\mathcal{V}_i}, \overline{P^{\mathrm{g}}_i}, \overline{Q^{\mathrm{g}}_i} \tag{1f}$$

$$\underline{\tilde{P}^{\mathrm{g}}_i}, \underline{\tilde{Q}^{\mathrm{g}}_i} \le \tilde{P}^{\mathrm{g},c}_{i,t}, \tilde{Q}^{\mathrm{g},c}_{i,t} \le \overline{\tilde{P}^{\mathrm{g}}_i}, \overline{\tilde{Q}^{\mathrm{g}}_i} \tag{1g}$$

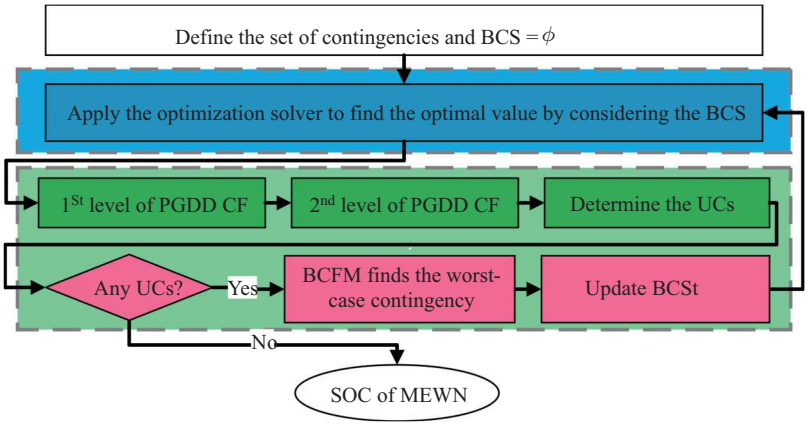

Fig. 1. Procedure to obtain the SOC-MEWN.

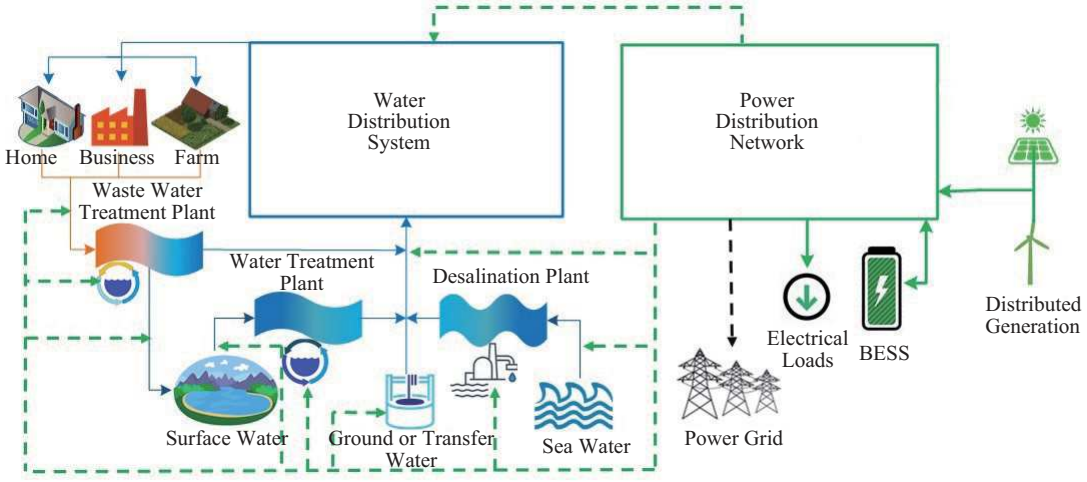

Fig. 2. Schematic of a typical MEWN.

$$\begin{cases} \widehat{\mathcal{V}} + z_{ij}^2 \mathcal{I}_{ij,t}^c = 2(r_{ij} P_{ij,t}^c + x_{ij} Q_{ij,t}^c), & \text{if } \mu_{ij}^c = 1 \\ \mathcal{I}_{ij,t}^c, P_{ij,t}^c, Q_{ij,t}^c = 0 & \text{if } \mu_{ij}^c = 0 \end{cases} \tag{1h}$$

$$\sum_{(i,j)} \mu_{ij}^c + 1 = N_{\mathrm{B}} \tag{1i}$$

where $\widehat{\mathcal{V}} = \mathcal{V}_{i,t}^c - \mathcal{V}_{j,t}^c$. Constraints (1a) and (1b) denote the nodal balance of active and reactive power, respectively. $P_{i,t}^{\mathrm{g}}$ and $Q_{i,t}^{\mathrm{g}}$ include the grid power at the substation bus and controllable DG power. Without controllable DGs, we only have $P_{1,t}^{\mathrm{g}}$ and $Q_{1,t}^{\mathrm{g}}$, which represent power from the grid via PCC. The secondary CAs $\tilde{P}_{i,t}^{g,c}$ and $\tilde{Q}_{i,t}^{g,c}$ are permissible changes in the active and reactive grid/controllable DG power, respectively. Constraints (1c) to (1e) are related to Ohm's law; and (1f) to (1g) describe upper and lower bounds of variables. Constraints (1h) to (1i) are related to distribution network reconfiguration. The value of the binary variable μ_{ij}^c is 1 if the switch status of the reserve line between bus i and bus j is closed.

B. Water Distribution System

This section describes the WDS model which consists of mass flow conservation law, pipe network, water tank, pressure-reducing valve, and water pump model.

1) Mass Flow Conservation Law

WDS must conserve total mass flow rate at every node. This law is modeled by (2a) to (2b):

$$\sum_{m} f_{nm,t}^c = F^{\mathrm{R}} + \tilde{F}_{n,t}^{\mathrm{R},c} - d_{n,t} + F_{n,t}^{\mathrm{T},c} \tag{2a}$$

$$\underline{F_n^{\mathrm{R}}}, \underline{F_n^{\mathrm{T}}}, \underline{f_{nm}} \le F_{n,t}^{\mathrm{R}}, F_{n,t}^{\mathrm{T},c}, f_{nm,t}^c \le \overline{F_n^{\mathrm{R}}}, \overline{F_n^{\mathrm{T}}}, \overline{f_{nm}} \tag{2b}$$

where (2a) guarantees the node's total water injection equals its total water output.

2) Pipe Network

There are several formulas to model the water pipe network. In this paper, we use the Darcy-Weisbach formula which is the most theoretically accurate one [18]:

$$\widehat{Y} = R_{nm}^{\mathrm{w}} \operatorname{sgn}(f_{nm,t}^c)(f_{nm,t}^c)^2 \tag{3a}$$

$$\begin{cases} \widehat{Y} + y_{nm,t}^{\mathrm{G},c} = R_{nm}^{\mathrm{w}} (f_{nm,t}^c)^2 & \text{if pump is ON} \\ f_{nm,t}^c = 0 & \text{if pump is OFF} \end{cases} \tag{3b}$$

$$\underline{y_n^c} \le y_{n,t}^c \le \overline{y_n^c} \tag{3c}$$

$$R_{nm}^{\mathrm{w}} \times \pi^2 g D_{nm}^5 = 8 f_{\mathrm{s}} L_{nm} \tag{3d}$$

where $\widehat{Y} = y_{n,t}^c - y_{m,t}^c + h_{nm}$. Constraints (3a) and (3b) show the head lost along a regular pipe and a pump, respectively.

3) Water Tank

To model water tanks, we consider each tank as a node and use the following formulas [19]:

$$y_{n,t+1}^{\mathrm{T},c} = y_{n,t}^{\mathrm{T},c} + \frac{F_{n,t}^{\mathrm{T},c}}{A_n^{\mathrm{T}}} \tag{4a}$$

$$V_{n,t+1}^{\mathrm{T},c} = V_{n,t}^{\mathrm{T},c} + F_{n,t}^{\mathrm{T},c} \tag{4b}$$

$$V_{n,0}^{\mathrm{T},c} = V_{n,24}^{\mathrm{T},c} \tag{4c}$$

$$\underline{V_n^{\mathrm{T}}} \le V_{n,t}^{\mathrm{T},c} \le \overline{V_n^{\mathrm{T}}} \tag{4d}$$

Constraint (4a) describes head pressure change at the node of the water tank; (4b) shows stored water in the water tank at each time slot; and (4c) represents the daily water input to the tank should be equal to daily water output from it.

4) Pressure-Reducing Valve

There are several types of controllable valves that can help operators control water flows in WDSs [20]. In this paper, we assume the system operators use pressure-reducing valves to control water head pressure, and the mathematical model is given by:

$$-PR \le y_{n,t}^c - y_{m,t}^c + h_{nm} \le PR \tag{5}$$

C. Electricity-driven Water Facilities

We consider fixed-speed pumps as an EDWF which can be modeled by a quadratic function of water flow [21]:

$$\eta P_{i,t}^{\mathrm{pump},c} = 2.725 \times (a_1 (f_{nm,t}^c)^2 + a_0 f_{nm,t}^c) \tag{6}$$

D. Objective Function

This subsection introduces an optimization framework for secure operation of MEWN based on the mathematical model. The objective of this problem is to minimize total energy cost of meeting electricity and water demands.

$$Cost = \sum_t \left(\rho_t^{\mathrm{G}} P_{1,t}^g + \sum_{i \in B \setminus B_{\mathrm{s}}} \rho_{1,i} P_{i,t}^{\mathrm{g}} + \rho_{2,i} {P_{i,t}^{\mathrm{g}}}^2 \right) \tag{7}$$

where the first term relates to grid power costs, and second relates to controllable DGs power costs. ρ_t^{G} is obtained by solving economic dispatch. The SOC-MEWN model is:

$$\begin{aligned} &\min \quad (7) \\ &\text{s.t.} \quad (1)\text{–}(6). \end{aligned} \tag{8}$$

We have proposed the required energy is supplied by the power grid, controllable DGs, and renewable energy resources.

III. Solution Method

This section introduces the proposed solution method for solving the SOC-MEWN problem. First, we discuss convex relaxation for the nonconvex MEWN model. Then, we explain the proposed PGDD-CF method for reducing computational burden of the SOC-MEWN problem.

A. Convex-Hull Relaxation of Nonlinear Components

In this subsection, we convexify formulation of the MEWN to mitigate computational burden. We relax constraint (1d) by using the convex hull relaxation model represented in [22]:

$$(P_{ij,t}^c)^2 + (Q_{ij,t}^c)^2 \le \mathcal{V}_{i,t}^c \mathcal{I}^c{}_{ij,t} \tag{9a}$$

$$\underline{\mathcal{V}_i} \overline{\mathcal{V}_i} \mathcal{I}^c{}_{ij,t} + \overline{S_{ij}}^2 \mathcal{V}_{i,t}^c \le \overline{S_{ij}}^2 (\underline{\mathcal{V}_i} + \overline{\mathcal{V}_i}) \tag{9b}$$

The big-M technique is applied to eliminate the logic proposition. Constraint (1h) is replaced by (10a) to (10b), and (10d) to (10f) show the convex model of (3b).

$$\widehat{\mathcal{V}} + z_{ij}^2 \mathcal{I}_{ij,t}^c - 2(r_{ij} P_{ij,t}^c + x_{ij} Q_{ij,t}^c) \ge M(\mu_{ij}^c - 1) \tag{10a}$$

$$\widehat{\mathcal{V}} + z_{ij}^2 \mathcal{I}_{ij,t}^c - 2(r_{ij} P_{ij,t}^c + x_{ij} Q_{ij,t}^c) \le M(1 - \mu_{ij}^c) \tag{10b}$$

$$0 \le P^c_{ij,t}, Q^c_{ij,t}, \mathcal{I}^c_{ij,t} \le \mu^c_{ij}\overline{P_{ij}}, \mu^c_{ij}\overline{Q_{ij}}, \mu^c_{ij}\overline{\mathcal{I}_{ij}} \tag{10c}$$

$$\widehat{Y} + y^{\mathrm{G},c}_{nm,t} - R^{\mathrm{w}}_{nm}(f^c_{nm,t})^2 \ge M(\alpha^{\mathrm{p}}_{nm,t} - 1) \tag{10d}$$

$$\widehat{Y} + y^{\mathrm{G},c}_{nm,t} - R^{\mathrm{w}}_{nm}\overline{f}_{nm} f^c_{nm,t} \le M(1 - \alpha^{\mathrm{p}}_{nm,t}) \tag{10e}$$

$$0 \le f_{nm} \le \alpha^{\mathrm{p}}_{nm,t}\overline{f}_{nm} \tag{10f}$$

Constraint (11) shows a quasi-convex hull of (3a) [23]:

$$\widehat{Y}\begin{cases} \le (\sqrt{8}-2)R^{\mathrm{w}}_{nm}\overline{f}_{nm} f^c_{\mathrm{mn,t}} + (3-\sqrt{8})R^{\mathrm{w}}_{nm}\overline{f}^2_{nm} \\ \ge (\sqrt{8}-2)R^{\mathrm{w}}_{nm}\underline{f}_{nm} f^c_{nm,t} - (3-\sqrt{8})R^{\mathrm{w}}_{nm}\underline{f}^2_{nm} \\ \ge 2R^{\mathrm{w}}_{nm}\overline{f}_{nm} f^c_{nm,t} - R^{\mathrm{w}}_{nm}\overline{f}^2_{nm} \\ \le 2R^{\mathrm{w}}_{nm}\underline{f}_{nm} f^c_{nm,t} + R^{\mathrm{w}}_{nm}\underline{f}^2_{nm} \end{cases} \tag{11}$$

A quadratic equation like (6) can be relaxed as the intersection of a concave inequality and a convex inequality. Equation (12) represents the convex model of (6).

$$\eta P^{\mathrm{pump}}_{i,t} \ge 2.725 \times (a_1(f_{nm,t})^2 + a_0 f_{nm,t}) \tag{12a}$$

$$\eta P^{\mathrm{pump}}_{i,t} \le 2.725 \times (a_1\overline{f}_{nm} + a_0) f_{nm,t} \tag{12b}$$

B. Physic-Guided Data-Driven Contingency Filtering

This section introduces the proposed PGDD-CF method which is used to find worst-case contingencies. Most contingencies are redundant for security operations in real-world systems, so only a subset of contingencies must be taken into account. As this set of contingencies covers approximately the entire contingencies, optimal value for the base-case operation subject to this subset of contingencies will also be the optimal value for the original problem. To determine this subset of contingencies, we have developed a hybrid physics and data-driven CF method, consisting of two modules. Historical contingencies resulting from offline optimization problems are trained using the PGDD approach. Contingencies are classified into three categories based on the trained hypothesis function: low violation contingencies (LVCs), medium violation contingencies (MVCs), and high violation contingencies (HVCs). Primary CAs can eliminate violations of LVCs. While the secondary CA can address some MVCs, other MVCs may need preventive action to avoid any violation. By checking feasibility of MVCs with (1)–(6), UCs can be found. A feasibility check for LVCs is not required because LVC violation is low and can be simply mitigated by primary CAs. A feasibility check is also unnecessary for HVCs as they cannot be addressed through corrective and preventative actions, and hardening is necessary to avoid this type of contingency. In the second module, the highest violation in the group of UCs is identified as the worst-case contingency. The worst-case contingency is added to the BCS, and the next iteration begins. The procedure will continue until there are no UCs. Algorithm 1 illustrates the proposed CF method. The following subsections provide more details about the proposed hybrid physics and data-driven CF method.

Algorithm 1: ML-Enhanced Online Mixed-Integer Optimization

1. Define the initial binding contingencies set (BCS $= \varnothing$);
2. Apply the optimization solver to obtain the SOC-MEWN and find the optimal value of $P^{g*}_{i,t}$, $Q^{g*}_{i,t}$, $F^{R*}_{n,t}$ and $\alpha^{\mathrm{P}*}_{nm,t}$ subject to the network constraints in the base-case operation and BCS
3. Build the dynamic data set based on the physical information
4. PGDD predicts the network configuration utilizing input data and the first-level hypothesis functions
5. Build the filtered data set
6. Define the initial sets (LVC $= \varnothing$, MVC $= \varnothing$, HVC $= \varnothing$);
7. PGDD categorizes all contingencies as HVC, MVC, and LVC by applying the hybrid physics and data-driven method;
8. Check the feasibility of MVC set by using (1)–(6).
9. **if** *there are any UCs in the set of MVCs* **then**
10. BCFM finds the **worst-case contingency** among UCs by using (1c), (1e)–(1g), (2b), (3c), (4), (5), (9)–(12), and (25)
11. BCS $\leftarrow$ BCS $+$ **worst-case contingency**
12. **goto** step **2**
13. **else**
14. Optimal solution
15. **end**

1) Physic-guided data-driven module

We propose a two-level learning approach involving data-driven and physics-based methods to find UCs. An appropriate training data set is required for any learning approach. However, historical measurements of optimal values of power generation and water production under different power and water demands in real-world applications are generally not available. Moreover, data on which contingencies lead to system failure and which one is controllable in terms of power demand, water demand, power generation, and water production may not be available either. Therefore, we utilize historical 24-hour load profiles and solve related offline optimization problems to build the training static data set. The proposed method may need more iterations to find UCs if the training data set lacks sufficient reliability. Therefore, there should be sufficient offline optimization problems to obtain a reliable training data set with high accuracy in the hypothesis function. In the future, such data sets can be obtained by data acquisition systems without solving any offline optimization problems. To find violation of each contingency, we add new variables $\tilde{P}^{\mathrm{p},c}_{i,t}$, $\tilde{P}^{\mathrm{n},c}_{i,t}$ and $\tilde{d}^{\mathrm{p},c}_{n,t}$, $\tilde{d}^{\mathrm{n},c}_{n,t}$ to (1a), (1b), and (2a), and write them as (13), (14), and (15), respectively.

$$P^{\mathrm{g}}_{i,t} - P^{\mathrm{L}}_{i,t} + \tilde{P}^{\mathrm{p},c}_{i,t} - \tilde{P}^{\mathrm{n},c}_{i,t} = r_{ij}\mathcal{I}^c_{ij,t} - P^c_{ji,t} + \sum_k P^c_{ki,t} \tag{13}$$

$$Q^{\mathrm{g}}_{i,t} - Q^{\mathrm{L}}_{i,t} + \tilde{Q}^{\mathrm{p},c}_{i,t} - \tilde{Q}^{\mathrm{n},c}_{i,t} = x_{ij}\mathcal{I}^c_{ij,t} - Q^c_{ji,t} + \sum_k Q^c_{ki,t} \tag{14}$$

$$\sum_l f^c_{nl,t} = F^{\mathrm{R}}_{n,t} - d_{n,t} + \tilde{d}^{\mathrm{p},c}_{n,t} - \tilde{d}^{\mathrm{n},c}_{n,t} + F^{\mathrm{T},c}_{n,t} \tag{15}$$

The objective function of the optimization problem is to minimize violation of each contingency [6], [12]:

$$\gamma^c = \sum_{i,n,t}\left(\omega_i \frac{\tilde{P}^{\mathrm{p},c}_{i,t} + \tilde{P}^{\mathrm{n},c}_{i,t}}{P^{\mathrm{l}}} + \omega_n \frac{\tilde{d}^{\mathrm{p},c}_{n,t} + \tilde{d}^{\mathrm{n},c}_{n,t}}{d}\right) \tag{16}$$

Some loads, such as hospitals, have higher importance than other loads, meeting which is a top priority. We can attribute a weight to each bus and node to account for importance of loads. Constraints of this objective function are (1c), (1e)–(1g),

(2b), (3c), (4), (5), and (9)–(15). Now, the training static data set is created as follows:

$$\Gamma^S = \left\{(\kappa_1^S, \psi_1^S), (\kappa_2^S, \psi_2^S), \cdots, (\kappa_{N_{\rm ds}}^S, \psi_{N_{\rm ds}}^S)\right\} \tag{17}$$

where $\psi_k^S = \{\gamma_k^S, \mu_k^S\}$ represents output including the violation and network configuration, and $\kappa_k^S = \{P_{i,t}^{{\rm l},k}, Q_{i,t}^{{\rm l},k}, d_{n,t}^k, P_{i,t}^{g*,k}, Q_{i,t}^{g*,k}, F_{n,t}^{R*,k}, \alpha_{nm,t}^{P*,k}, c^k\}$ shows input data, where $P_{i,t}^{g*,k}$, $Q_{i,t}^{g*,k}$, $F_{n,t}^{R*,k}$ and $\alpha_{nm,t}^{P*,k}$ are optimal values of decision variables for $k^{\rm th}$ data. To make the training data set more efficient, we modify historical data with physical information to create a dynamic data set. On days with similar environmental data, such as temperature, wind speed, and weather, the power system may operate similarly. For example, the allowed power flow will be lower on a hot day with low wind speed than on a cold day with high wind speed. In addition, on sunny days, there is a significant potential for generating power from photovoltaic cells. In sunny weather, we can use this power to mitigate some contingencies and decrease value of the violation, but in cloudy weather, we are limited in our options. Therefore, the physical situation, such as wind speed, temperature, and weather conditions, can change the violation of one specific contingency. We propose building a dynamic data set by considering physics information. A specific weather condition is given to the weighting function to account for wind speed (low, moderate, and high), temperature (hot, mild, and cold), and weather conditions (sunny, cloudy, and snowy). The dynamic data set will be created by weighting the static data set.

$$\begin{aligned}\Gamma^{\rm D} &= \left\{\omega_1^{\rm Ph}(\kappa_1^S, \psi_1^S), \omega_2^{\rm Ph}(\kappa_2^S, \psi_2^S), \cdots, \omega_{N_{\rm ds}}^{\rm Ph}(\kappa_{N_{\rm ds}}^S, \psi_{N_{\rm ds}}^S)\right\} \\ &= \left\{\left(\kappa_k^{\rm D}, \psi_k^{\rm D}\right)\right\},\ k = 1, \cdots, N_{\rm ds} \end{aligned} \tag{18a}$$

$$\omega_k^{\rm Ph} = \omega_k^{\rm temp} + \omega_k^{\rm wind} + \omega_k^{\rm weather} \tag{18b}$$

where $\omega_k^{\rm temp}$, $\omega_k^{\rm wind}$, and $\omega_k^{\rm weather}$ can be three different values based on physical information. For example, there are three categories of wind speed: high wind speed, moderate wind speed, and low wind speed.

$$\omega_k^{\rm wind} = \begin{cases} \vartheta_1^{\rm wind}, & \text{if same class,} \\ \vartheta_2^{\rm wind}, & \text{if adjacent classes,} \\ \vartheta_3^{\rm wind}, & \text{if non-adjacent classes} \end{cases} \tag{19}$$

where, for a specific case, exact values of $\vartheta_1^{\rm wind}$, $\vartheta_2^{\rm wind}$, and $\vartheta_3^{\rm wind}$ can be determined by experience of the system operators. $\omega_k^{\rm wind}$ is equal to $\vartheta_1^{\rm wind}$ if the wind speed class of inputted physical information and $k^{\rm th}$ data point match. If their classes are adjacent, it will be $\vartheta_2^{\rm wind}$, and if they are not adjacent, it will be $\vartheta_3^{\rm wind}$. The situation is the same for $\omega_k^{\rm temp}$ and $\omega_k^{\rm weather}$. Accordingly, the maximum value of $\omega_k^{\rm Ph}$ occurs when classes of wind speed, temperature, and weather are the same as classes of physical information. Using supervised ML, we have explored the relationship between input data and output data:

$$\mathscr{F}_{\rm firstlevel}(\kappa_k^{\rm D}) = \psi_k^{\rm D},\ \forall k \in \{1, 2, \cdots, N_{\rm ds}\}, \tag{20}$$

where $\psi_k^{\rm D} = \{\gamma_k^{\rm D}, \mu_k^{\rm D}\}$ shows output data, and $\kappa_k^{\rm D} = \kappa_k^S$ represents input data in the dynamic training data set. The first level of the PGDD-CF method will map input data to the network configuration ($\mu^{\rm First}$) and violation ($\gamma^{\rm First}$). A filter function is applied following the first level, which uses the obtained configuration of the network and dynamic data set to produce a filtered data set. This function filters data with similar configuration to provide the filtered data set:

$$\begin{aligned}\Gamma^{\rm F} &= \left\{\omega_1^F(\kappa_1^S, \psi_1^S), \omega_2^F(\kappa_2^S, \psi_2^S), \cdots, \omega_{N_{\rm ds}}^F(\kappa_{N_{\rm ds}}^S, \psi_{N_{\rm ds}}^S)\right\} \\ &= \left\{(\kappa_k^{\rm F}, \psi_k^{\rm F})\right\},\ k = 1, \cdots, N_{\rm ds} \end{aligned} \tag{21a}$$

$$\omega_k^F = \begin{cases} 0, & \text{if } \mu_k^{\rm D} \neq \mu^{\rm First} \\ 1, & \text{if } \mu_k^{\rm D} = \mu^{\rm First} \end{cases} \tag{21b}$$

where $\psi_k^{\rm F} = \gamma_k^{\rm F}$ and $\kappa_k^{\rm F} = \kappa_k^S$ represent output and input data of the filtered training data set, respectively. In the second level, the hypothesis function maps input data to the second level violation ($\gamma^{\rm Second}$) based on the filtered data set.

$$\mathscr{F}_{\rm secondlevel}(\kappa_k^{\rm F}) = \psi_k^{\rm F}. \tag{22}$$

When violations of both levels are found, the final violation is calculated by weighting the predicted violations:

$$\gamma^{\rm Ph} = \omega^{\rm First} \times \gamma^{\rm First} + \omega^{\rm Second} \times \gamma^{\rm Second} \tag{23}$$

A high value of $\omega^{\rm First}$ encourages the PGDD to learn from empirical knowledge, while a high value of $\omega^{\rm Second}$ encourages the PGDD to respect physical knowledge. The architecture of the PGDD method, which is related to steps 3 to 8 of Algorithm 1, is illustrated in Fig. 3. In the first level, the dynamic data set guides the hypothesis function to map input data to network configuration and first-level violation. The second level uses network configuration obtained in the first level to refine the dynamic data set and create the filtered data set. The filtered data set guides the hypothesis function of the second level and maps input data to the second-level violation. Lastly, first- and second-level violations are combined to determine the final violation for contingency classification. The PGDD classifies contingencies into three categories based on their violations:

$$\text{Contingency Class} = \begin{cases} \text{LVC}, & \text{if } \gamma^{\rm P} \leq \xi^{\rm LM} \\ \text{MVC}, & \text{if } \xi^{\rm LM} \leq \gamma^{\rm P} \leq \xi^{\rm MH} \\ \text{HVC}, & \text{if } \xi^{\rm MH} \leq \gamma^{\rm P} \end{cases} \tag{24}$$

The flowchart in Fig. 4 illustrates the logic of contingency classification based on the proposed method. The first level is shown in red, second level is shown in blue, and input data is shown in green. The first five steps of the proposed method, which relate to the first level, consider the optimal values of decision variables of the master problem to obtain first-level violation and network configuration in step 4. Using the dynamic data set created in step 2 and network configuration, step 6 constructs the filtered data set. Step 8 finds the second violation based on input data. Finally, the contingency class is determined after considering both violations in step 10.

We apply DT, SVM, NB, and KNN to train $\Gamma^{\rm D}$ and $\Gamma^{\rm F}$, and examine their accuracy to find the most efficient one for determining the UCs. The PGDD evaluates feasibility using the optimal solution provided in the second step of the algorithm for different contingencies following contingency classification. The LVC can be addressed with primary CA so the optimal solution of the second step is feasible for any LVC.

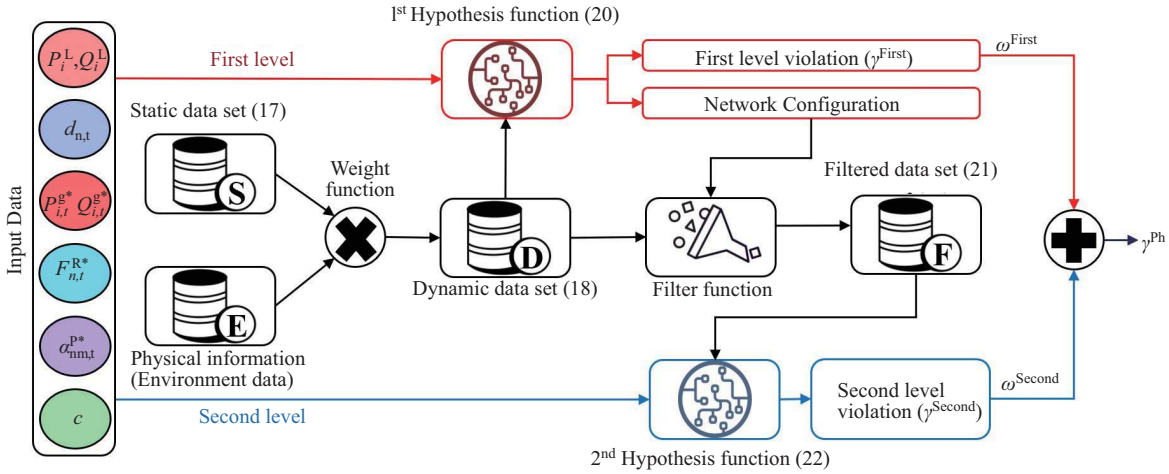

Fig. 3. PGDD-CF method: — first level, — second level, — data sets: the environment data includes temperature, wind speed, and weather conditions.

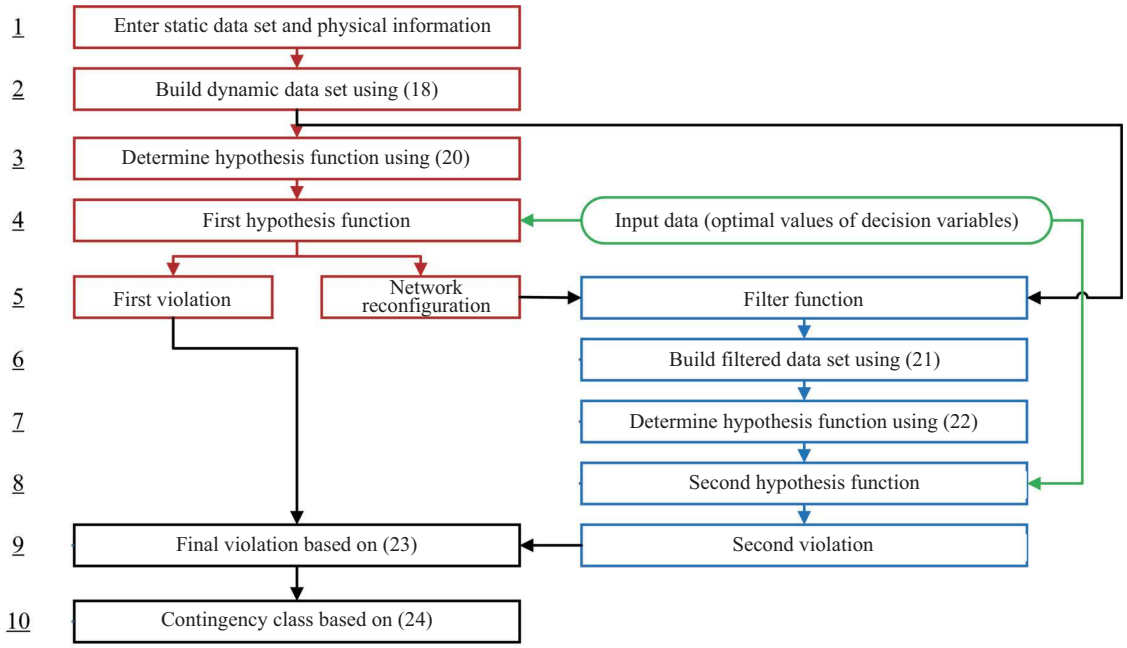

Fig. 4. Logic explanation for contingency classification based on the proposed method

HVCs cannot be controlled with preventive and corrective action, so hardening is proposed to prevent occurrence of this type of contingencies. Thus, to determine UCs, only MVCs need to be checked. Optimal values of the second step in Algorithm 1 are used to check feasibility of constraints (1)–(6). As long as optimal values satisfy all constraints, the operator can eliminate the violation by applying CAs. Consequently, the PGDD first classifies contingencies into three classes and then finds the UCs among MVCs.

2) Binding Contingency Filtering Module

BCFM solves the optimization problem for all UCs and finds the worst-case contingency which will be added to the master problem. This optimization problem includes violation, and CAs at the same time, where (1a), (1b), and (2a) are replaced by (25a), (25b), and (25c), respectively.

$$P^{\mathrm{g}}_{i,t} + \tilde{P}^{\mathrm{g},c}_{i,t} - P^{\mathrm{L}}_{i,t} + \tilde{P}^{\mathrm{p},c}_{i,t} - \tilde{P}^{\mathrm{n},c}_{i,t} = r_{ij}\mathcal{I}^{c}_{ij,t} - P^{c}_{ji,t} + \sum_{k} P^{c}_{ki,t} \tag{25a}$$

$$Q^{\mathrm{g}}_{i,t} + \tilde{Q}^{\mathrm{g},c}_{i,t} - Q^{\mathrm{L}}_{i,t} + \tilde{Q}^{\mathrm{p},c}_{i,t} - \tilde{Q}^{\mathrm{n},c}_{i,t} = x_{ij}\mathcal{I}^{c}_{ij,t} - Q^{c}_{ji,t} + \sum_{k} Q^{c}_{ki,t} \tag{25b}$$

$$\sum_{m} f^{c}_{nm,t} = F^{\mathrm{R}}_{n,t} + \tilde{F}^{\mathrm{R},c}_{n,t} - d_{n,t} + \tilde{d}^{\mathrm{p},c}_{n,t} - \tilde{d}^{\mathrm{n},c}_{n,t} + F^{\mathrm{T},c}_{n,t} \tag{25c}$$

The objective function of BCFM is (16), and constraints are (1c), (1e)–(1g), (2b), (3c), (4), (5), (9)–(12), and (25). The worst-case contingency is the contingency with the highest violation. This contingency is added to the BCS, and then the algorithm returns to its second step to start the next iteration. Algorithm 1 reaches the optimal solution when there is no UC.

IV. Case Studies

Based upon the different characterizations of the PDN and WDS in different areas [15], [24], we demonstrate robustness of the proposed method by examining it on two test systems. The first test case is the modified IEEE 13-bus system with 8-node EPANET WDS which represents the MEWN of small communities, such as industrial parks. The second one is the IEEE 33-bus system with 13-node Otsfeld WDS, which is a bigger system and represents the MEWN of city scale. A large-scale energy and water system operates as two separate entities, and conflicts appear between them. Consequently, our method, even though mathematically applicable to larger systems, cannot be used to get optimal operation for both systems due to existing conflicts. A 24-hour nodal price and a load curve of power demand [25], [26], excluding water pumps demand, are used to find the solution to the SOC-MEWN problem. Fig. 5(a) shows nodal price and two typical load curves for two different case studies. Training data sets are built based on load curves from PJM [26] shown in Fig. 5(b). For each case study, we have used these load curves and solved related offline optimization problems to build the training data set. The same priority is given to all buses and nodes by applying equal weight factors. Since real environmental data are not available, we did not consider them and related weight factors are considered the same. The training data set is used to fit parameters of four different supervised methods, namely DT, KNN, SVM, and NB. A test data set related to the first case study with 96 contingencies is employed for testing these supervised learning methods for the first level of our PGDD method. Fig. 6 and Table I show accuracy of these methods for contingency classification at the first level. The DT method has a 95.83% accuracy rate which is higher than other methods, and therefore it is chosen as the supervised learning approach for contingency classification. In case of an inaccurate hypothesis function, more iterations will be required to reach all UCs. The proposed method guarantees MEWN's security even when it is highly computational. Another test data set including 256 contingencies from the second case study is used to compare the pure ML classification with our proposed PGDD method. Fig. 7 illustrates the PGDD method improves classification accuracy from 91.8% to 99.2%. There are 21 wrong predictions in the first level (Fig. 7(a)). In the second level, wrong predictions are reduced to two after adding network configuration and using hybrid physics and data-driven methods (Fig. 7(b)).

TABLE I
Accuracy of Different Supervised Learning Methods in CF

Supervised learning method	Wrong Prediction		Accuracy (%)
	LVC	MVC	
DT	1	3	95.83
KNN	21	–	78.12
SVM	12	9	78.12
NB	77	–	19.79

We examine the case studies, explain numerical results (all simulations are run on Intel (R) Core (TM) i7-9700 CPU 3 GHz with 16 GB RAM), and compare our CF method to other existing CF methods in the following subsections.

A. IEEE 13-bus ADN with 8-node EPANET WDS

We have executed the proposed method on a MEWN, as shown in Fig. 8, which consists of a modified IEEE 13-bus system with an 8-node EPANET water system [27] that can be used for a MEWN in a small community such as industrial parks. The PGDD module needs optimal values of normal operation to classify contingencies and determine the UCs. According to the PGDD, 12 contingencies fit into three categories: 0 HVC, 1 MVC, and 11 LVCs. The only MVC can not be addressed with the CAs and needs preventive action. Fig. 9 shows results of PGDD for a single contingency in the first case study. For the next iteration, contingency 3 should be added to the master problem as worst-case contingency. The proposed method achieves SOC-MEWN after two iterations when contingency 3 is added to the BCS. Fig. 10 represents optimal values of grid/controllable DG power and water production for two iterations. MEWN secure operation costs $1751.4 per day, whereas independent secure operations of WDS and PDN would cost $1983.8 per day.

B. IEEE 33-bus ADN with the 13-node Otsfeld WDS

The IEEE 33-bus system and the 13-node Otsfeld regional WDS are considered for the second case study. The topology of the IEEE-33 bus distribution test system and the Otsfeld WDS are shown in Fig. 11. The IEEE 33-bus system can be used for an area of a city [28]. On the other hand, Wimmera Mallee Pipeline and Northern Mallee Pipeline are real

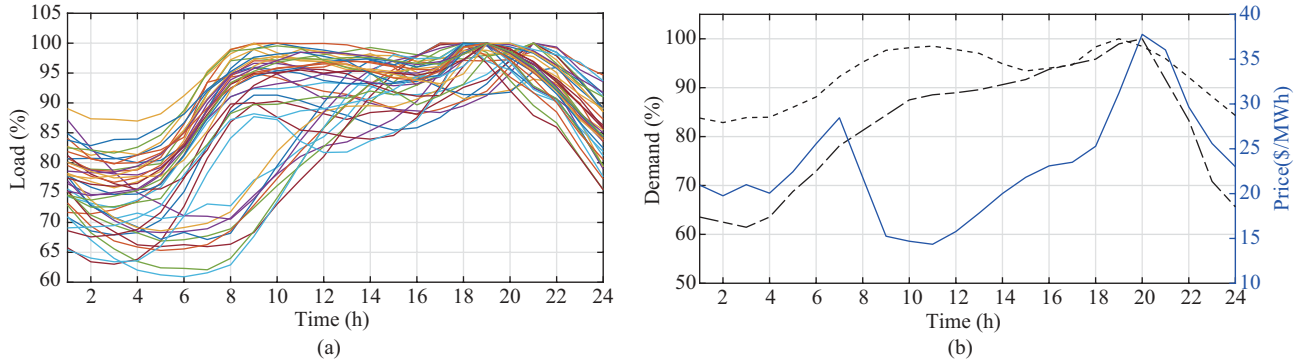

Fig. 5. Load curve and prices. (a) Different load curves from PJM to build the data set. (b) Load curves. –.–1st case study, – – 2nd case study, – hourly price.

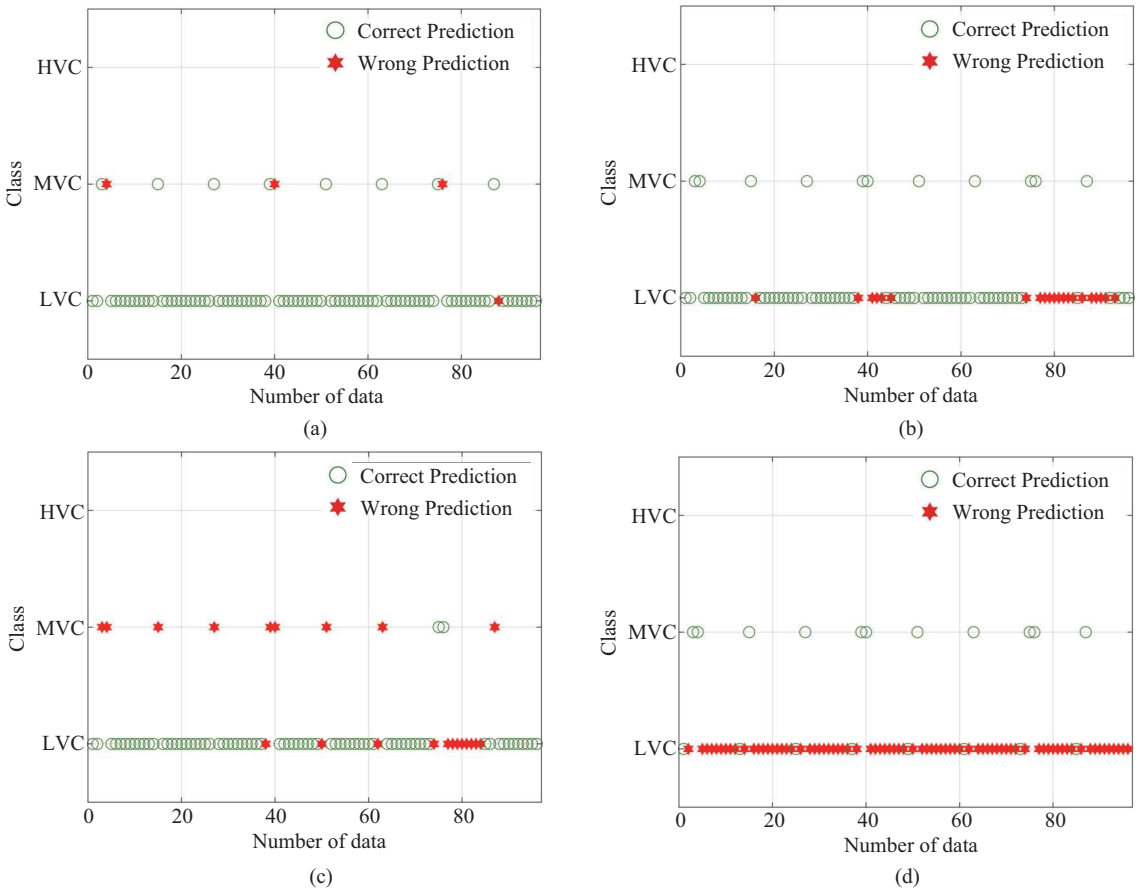

Fig. 6. Accuracy of different ML methods in contingency classification. (a) DT. (b) KNN. (c) SVM. (d) NB.

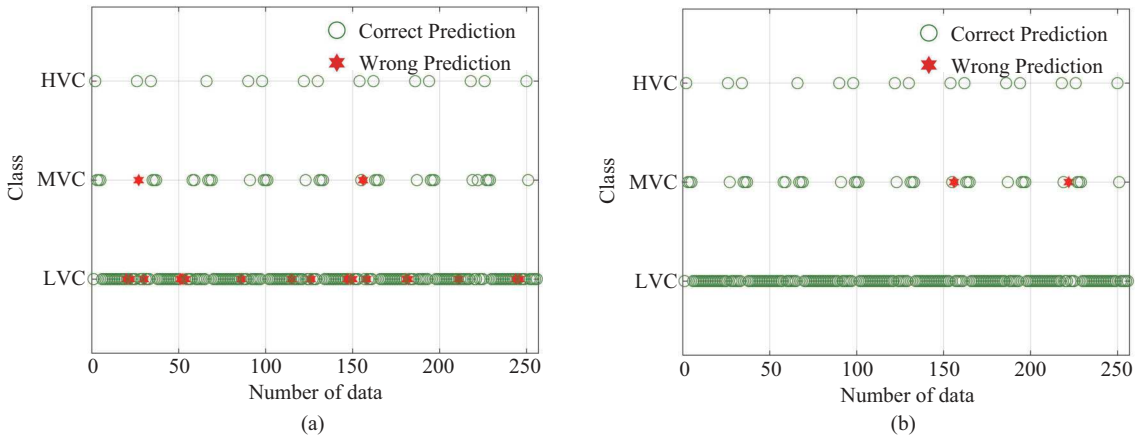

Fig. 7. Comparison between pure ML classification and PGDD classification. (a) Pure ML classification. (b) PGDD classification.

WDSs with Otsfeld network characteristics [29]. Therefore, these two systems can be considered for the same area. Three pumps acting as connectors between the WDS and the PDN are connected to buses 18, 25, and 33. The WDS consists of three water resources with three pump stations, two pressure-reducing valves (on pipes 6 and 10), and one water tank. Training data set Γ^{D} is built based on load curves shown in Fig. 5(b) for 32 contingencies. Optimal values for grid/controllable DG power and water production under normal operations are entered into the PGDD-CF method to find the worst-case contingency. The PGDD divides 32 contingencies into three categories: 5 HVCs, 3 MVCs, and 24 LVCs. Three MVCs are UC and need preventive action to address. PGDD results for a single contingency in the second case study are shown in Fig. 12. We suggest hardening lines 1, 2, 3, 4, and 26 to make sure HVC contingencies do not occur. BCFM finds contingency 5 as the worst-case contingency and adds it to the BCS to be considered in the master problem. There are no more UCs after applying contingency 5 to the master problem in the second iteration. Therefore, the

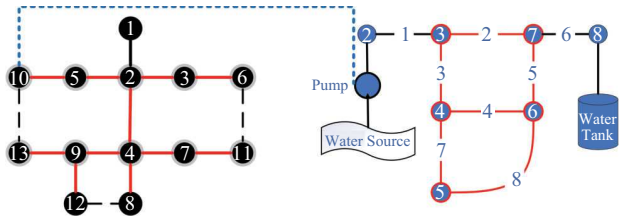

Fig. 8. IEEE 13-bus with EPANET 8-node.

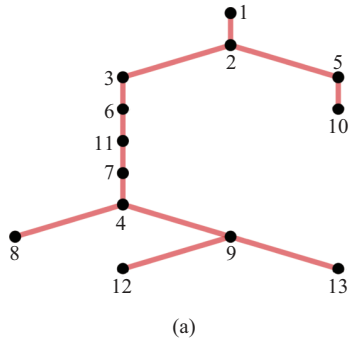

(a)

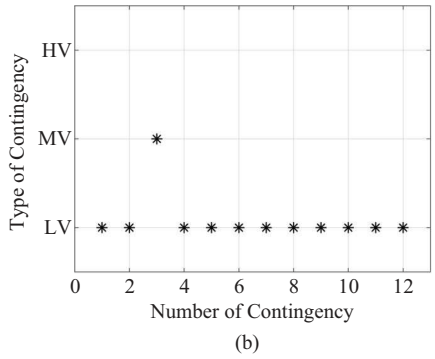

(b)

Fig. 9. 1st case study. (a) Network configuration. (b) Contingencies class.

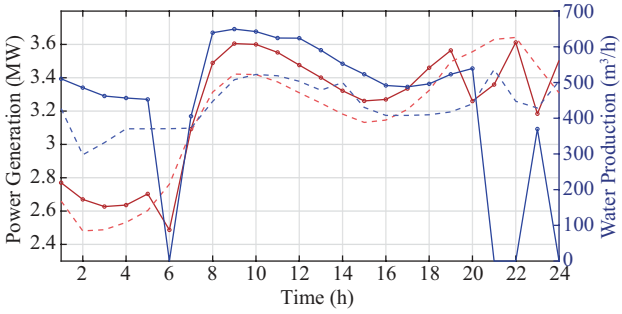

Fig. 10. The optimal value of power generation (red) and water production (blue) for the first case study: – – 1st iteration, – o –2nd iteration.

proposed method achieves SOC-MEWN after two iterations. Fig. 13 shows optimal values of grid/controllable DG power and water production for the first and second iterations. The secure operation cost will be decreased from \$886.1 per day to \$785.7 per day when the water and power systems work as a single integrated system.

C. Comparing with Other Contingency Filtering Methods

This section compares the PGDD-CF method with other existing CF methods. Existing CF methods, such as key

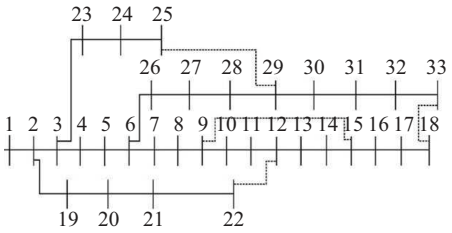

(a)

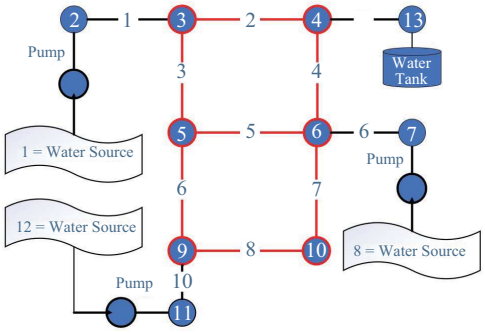

(b)

Fig. 11. Second test bed. (a) IEEE 33-bus system. (b) Otsfeld regional WDS.

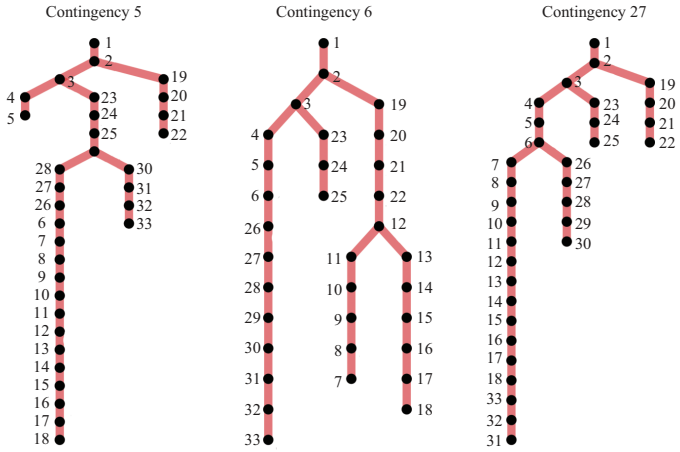

(a)

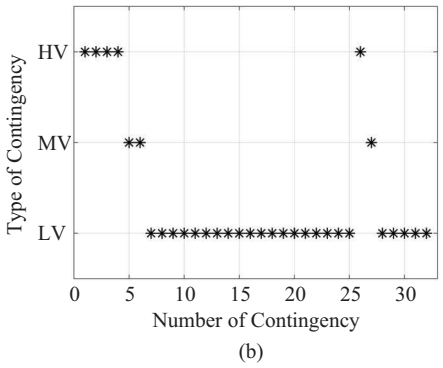

(b)

Fig. 12. 2nd case study. (a) Network configurations. (b) Contingencies class.

contingencies, require online optimization problems to be solved separately for each contingency in each iteration. The process is time-consuming, even when parallelized. The PGDD approach reduces the number of online optimization problems in the CF process. Data sets are built via offline

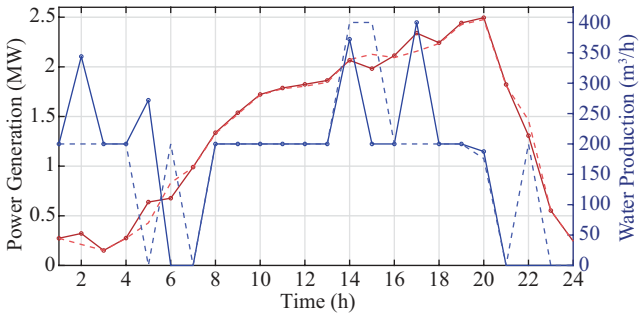

Fig. 13. The optimal value of power generation (red) and water production (blue) for the second case study: – – 1^{st} iteration, – o –2^{nd} iteration.

optimization, then DT parameters are fitted to the data to classify contingencies without requiring online optimization. A limited number of online optimization problems are then solved to find binding contingencies. Thus, each iteration is faster, resulting in quicker reach to the optimal solution. We apply the existing CF approach to our case studies to compare them with our proposed CF method, as shown in Table II. In the first case study, CF takes 10.52 seconds using the non-parallel manner and 3.202 seconds using the parallel manner. The proposed PGDD-CF method reduces this time to less than one second. Results of the second case study indicate CF time for the non-parallel manner, the parallel manner, and our method are 171.85 seconds, 15.43 seconds, and 1.12 seconds, respectively. As a result, our method speeds up the CF process.

TABLE II
SOLVER TIME FOR THE PGDD METHOD AND OTHER METHODS

Description	Case Study		Case 1	Case 2
First Iteration	Exiting Method	Non-Parallel	5.441	90.12
		Parallel	1.615	8.26
(s)	Our Method		0.689	0.746
Second Iteration	Exiting Method	Non-Parallel	5.075	81.73
		Parallel	1.578	7.17
(s)	Our Method		0.302	0.371
Total	Exiting Method	Non-Parallel	10.52	171.85
		Parallel	3.202	15.43
(s)	Our Method		0.991	1.117

V. CONCLUSION

We have developed a two-stage iterative algorithm, employing a hybrid physics and data-driven CF method, as well as the convexification technique to solve the SOC-MEWN problem. The CF method consists of two modules. The first module divides contingencies into three classes by applying PGDD to dynamic and filtered data sets resulting from offline optimization problems. Four supervised learning methods are examined, and DT is chosen as the most effective method for contingency classification. Once the contingencies have been classified, a feasibility check is conducted to identify UCs. The second module determines which UC is the worst-case contingency to add to the BCS for the next iteration. Once CAs can lead all contingencies to a feasible solution, iteration will end. Two case studies are used to validate effectiveness of our method. A comparison between our method and other existing CF methods shows our approach is faster than other methods. For two case studies, we achieve UCs in 0.99 seconds and 1.12 seconds, respectively. In contrast, it takes 10.52 seconds and 171.85 seconds for other existing CF methods.

REFERENCES

[1] T. Gonen, *Electric Power Distribution Engineering*, 3rd ed., Boca Raton: CRC Press, 2014.
[2] D. Jakus, R. Čađenović, J. Vasilj, and P. Sarajčev, "Optimal reconfiguration of distribution networks using hybrid heuristic-genetic algorithm," *Energies*, vol. 13, no. 7, pp. 1544, Mar. 2020.
[3] S. Babaei, R. W. Jiang, and C. Y. Zhao, "Distributionally robust distribution network configuration under random contingency," *IEEE Transactions on Power Systems*, vol. 35, no. 5, pp. 3332–3341, Sep. 2020.
[4] F. Capitanescu, J. L. M. Ramos, P. Panciatici, D. Kirschen, A. M. Marcolini, L. Platbrood, and L. Wehenkel, "State-of-the-art, challenges, and future trends in security constrained optimal power flow," *Electric Power Systems Research*, vol. 81, no. 8, pp. 1731–1741, Aug. 2011.
[5] G. Q. Sun, S. Chen, Z. N. Wei, K. W. Cheung, and H. X. Zang, "Corrective security-constrained optimal power and gas flow with binding contingency identification," *IEEE Transactions on Sustainable Energy*, vol. 11, no. 2, pp. 1033–1042, Apr. 2020.
[6] H. X. Yang and H. Nagarajan, "Optimal power flow in distribution networks under stochastic N-1 disruptions," *Electric Power Systens Research*, vol. 189, pp. 106689, Dec. 2020.
[7] R. Weinhold and R. Mieth, "Fast security-constrained optimal power flow through low-impact and redundancy screening," *IEEE Transactions on Power Systems*, vol. 35, no. 6, pp. 4574–4584, Nov. 2020.
[8] S. Fliscounakis, P. Panciatici, F. Capitanescu, and L. Wehenkel, "Contingency ranking with respect to overloads in very large power systems taking into account uncertainty, preventive, and corrective actions," *IEEE Transactions on Power Systems*, vol. 28, no. 4, pp. 4909–4917, Nov. 2013.
[9] A. Marano-Marcolini, F. Capitanescu, J. L. Martinez-Ramos, and L. Wehenkel, "Exploiting the use of DC SCOPF approximation to improve iterative AC SCOPF algorithms," *IEEE Transactions on Power Systems*, vol. 27, no. 3, pp. 1459–1466, Aug. 2012.
[10] Q. Y. Jiang and K. Xu, "A novel iterative contingency filtering approach to corrective security-constrained optimal power flow," *IEEE Transactions on Power Systems*, vol. 29, no. 3, pp. 1099–1109, May 2014.
[11] F. Bouffard, F. D. Galiana, and J. M. Arroyo, "Umbrella contingencies in security-constrained optimal power flow," in *Proceedings of the 15th Power Systems Computation Conference*, 2005, pp. 1–7.
[12] F. Capitanescu and L. Wehenkel, "A new iterative approach to the corrective security-constrained optimal power flow problem," *IEEE Transactions on Power Systems*, vol. 23, no. 4, pp. 1533–1541, Nov. 2008.
[13] A. S. Zamzam and N. D. Sidiropoulos, "Physics-aware neural networks for distribution system state estimation," *IEEE Transactions on Power Systems*, vol. 35, no. 6, pp. 4347–4356, Nov. 2020.
[14] O. A. Alimi, K. Ouahada, and A. M. Abu-Mahfouz, "A review of machine learning approaches to power system security and stability," *IEEE Access*, vol. 8, pp. 113512–113531, 2020.
[15] M. Goodarzi and Q. F. Li, "Evaluate the capacity of electricity-driven water facilities in small communities as virtual energy storage,"*Applied Energy*, vol. 309, pp. 118349, Mar. 2022.
[16] M. E. Baran and F. F. Wu, "Optimal capacitor placement on radial distribution systems, "*IEEE Transactions on Power Delivery*, vol. 4, no. 1, pp. 725–734, Jan. 1989.
[17] Q. F. Li, R. Ayyanar, and V. Vittal, "Convex optimization for des planning and operation in radial distribution systems with high penetration of photovoltaic resources," *IEEE Transactions on Sustainable Energy*, vol. 7, no. 3, pp. 985–995, Jul. 2016.
[18] L. A. Rossman *et al*., "Epanet users manual, an updated version," *US Environmental Protection Agency. Office of Research and Development*, 2020.
[19] M. Goodarzi, D. Wu, and Q. F. Li, "Fast security evaluation for operation of water distribution systems against extreme conditions," presented at the *2021 American Control Conference (ACC)*, 2021, pp. 3495–3500.
[20] D. Fooladivanda and J. A. Taylor, "Energy-optimal pump scheduling and water flow," *IEEE Transactions on Control of Network Systems*, vol. 5, no. 3, pp. 1016–1026, Sep. 2018.
[21] B. Ulanicki, J. Kahler, and B. Coulbeck, "Modeling the efficiency and power characteristics of a pump group," *Journal of Water Resources Planning and Management*, vol. 134, no. 1, pp. 88–93, Jan. 2008.

[22] Q. F. Li and V. Vittal, "Convex hull of the quadratic branch AC power flow equations and its application in radial distribution networks," *IEEE Transactions on Power Systems*, vol. 33, no. 1, pp. 839–850, Jan. 2018.
[23] Q. F. Li, S. Yu, A. S. Al-Sumaiti, and K. Turitsyn, "Micro water–energy nexus: Optimal demand-side management and quasi-convex hull relaxation," *IEEE Transactions on Control of Network Systems*, vol. 6, no. 4, pp. 1313–1322, Dec. 2019.
[24] M. Gilvanejad, M. Goodarzi, and H. Ghadiri, "Introduction of configurational indicators for distribution network optimality based on a zoning methodology," *AUT Journal of Electrical Engineering*, 2021.
[25] D. Narang and C. Neuman, "High penetration of photovoltaic generation study–flagstaff community power: Results of phase 1, "DOE Final Technical Report, de-ee0002060, Tech. Rep., 2011.
[26] Dataminer. (2022 Jan). [Online]. Available: https://dataminer2.pjm.com /feed/hrl_load_metered
[27] "Epanet 2: users manual," *US Environmental Protection Agency. Office of Research and Development, USA*, 2000.
[28] V. Vita, "Electricity distribution networks' analysis, with particular references to distributed generation and protection," Ph. D. dissertation, City University London, 2016.
[29] H. Mala-Jetmarova, A. Barton, and A. Bagirov, "Exploration of the trade-offs between water quality and pumping costs in optimal operation of regional multiquality water distribution systems," *Journal of Water Resources Planning and Management*, vol. 141, no. 6, pp. 04014077, Jun. 2015.

Mostafa Goodarzi received B.S. and M.S. degrees in Electrical Engineering from Amirkabir University of Technology, Tehran, Iran, in 2010 and 2012, respectively. He worked as a Research Engineer and Project Manager at Niroo Research Institute, Tehran, Iran, from 2012 to 2019. Currently, he is working as a Graduate Research and Teaching Assistant for the Department of Electrical and Computer Engineering, University of Central Florida, Orlando, FL, USA. His research interests include optimal operation and optimization methods, demand response, and application of Machine Learning in power and integrated systems.

Qifeng Li (SM'20) received a Ph.D. degree in Electrical Engineering from Arizona State University, Tempe, AZ, USA, in 2016. He is currently an Assistant Professor with the Department of Electrical and Computer Engineering, University of Central Florida (UCF), Orlando, FL, USA. Before joining UCF, he held a position of Postdoctoral Associate with the Department of Mechanical Engineering, Massachusetts Institute of Technology, Cambridge, MA, USA, from 2016 to 2018. His research interests include deterministic and uncertain optimization and nonlinear systems with applications in power and energy systems.